

SHIP-SHIP HYDRODYNAMIC INTERACTION IN CONFINED WATERS WITH COMPLEX BOUNDARIES BY A PANELLED MOVING PATCH METHOD

(DOI No: 10.3940/rina.ijme.2016.a1.339)

X-Q Zhou, S Sutulo, C Guedes Soares Centre for Marine Technology and Ocean Engineering (CENTEC), Instituto Superior Técnico, Universidade de Lisboa, Lisboa, Portugal

SUMMARY

This paper presents a potential flow solution for online estimation of hydrodynamic interaction between ships moving in restricted waters with complex boundaries. Each ship in concern is linked with a moving patch representing the arbitrary bathymetry beneath it. The wetted surfaces of ship hulls are meshed and loaded prior to the simulation, while the moving patches are dynamically discretized by a fast and robust mesh generator. The proposed method is validated for the ship-ship interaction case in the shallow water case with a flat and horizontal seabed where the mirror image technique is applicable, and satisfactory agreement is obtained. The method is further applied to simulate two interaction scenarios involving arbitrary seabed topography, and the numerical results are obtained and discussed.

NOMENCLATURE

A_w	Water plane area (m^2)
B	Beam of ship (m)
F	Force (N)
$G()$	Green's function
h	Water depth (m)
k	Number of images
L	Ship length (m)
M	Moment (N m)
N	Yaw moment (N m)
n	Outward unity normal
p	Pressure (Pa)
r	Velocity of yaw ($rad\ s^{-1}$)
S	Area of the total surface (m^2)
T	Draught (m)
t	Time (s)
u	Velocity of surge ($m\ s^{-1}$)
V	Velocity ($m\ s^{-1}$)
V_{cur}	Velocity of the current ($m\ s^{-1}$)
V_i	Induced velocity ($m\ s^{-1}$)
V_r	Relative velocity ($m\ s^{-1}$)
v	Velocity of sway ($m\ s^{-1}$)
X	Surge force (N)
Y	Sway force (N)
μ_{ij}	Added masses (kg; kg m)
ξ_i	Ship advance (m)
η_i	Ship transfer (m)
ρ	Density of fluid ($ton\ m^{-3}$)
σ	Source density
Φ	Total velocity potential ($m^2\ s^{-1}$)
ϕ	Perturbation potential ($m^2\ s^{-1}$)
ψ	Heading angle (rad)
Ω	Angular velocity ($rad\ s^{-1}$)

1. INTRODUCTION

The problem of the ship-ship hydrodynamic interaction in restricted waters has been increasingly attracting more attention than in open waters as nowadays the main dimensions of certain ship types are continuously getting larger and the water traffic is becoming busier in all harbours and canals throughout the world.

A large amount of researches have been done to investigate the ship-ship hydrodynamic interaction problem in confined waters. Most of them focused on shallow water of constant finite depth, while only a few dealt with complex water boundaries, more specifically, canals [1–3], rivers [4], and protruding or submerged banks [5].

Laforce et al. [1] presented experimental results of systematic captive model tests on three models of different lengths in open shallow and restricted water. The influence of the ship length, water depth and canal banks on hydrodynamic forces were discussed.

Kyulevcheliiev et al. [2] carried out a set of model experiments for the hydrodynamic effect of a moving ship on a stationary ship in restricted water. It was found that the wave effects might be significant at high ship speeds.

Experimental investigation of the hydrodynamic interaction between inland vessels during overtaking and encountering was conducted by Gronarz [4]. Original measurements with the data uncertainties and the propeller's influence were presented.

Vantorre et al [6] carried out a comprehensive set of ship-ship interaction tests involving four models with a variety of parametric configurations including lateral clearances, draughts, speeds and under-keel clearances. These experimental data were later used by Varyani and Vantorre [7] to compare with generic equations for the forces induced by a passing ship on a moored ship, and by Falter [8] to validate a potential-flow-based simulation code [9] for the

case of ship-ship interaction during overtaking and encounter manoeuvres in shallow waters .

Although experimental methods usually provide rather realistic and reliable estimates, but besides great financial cost and time consumption, they are of limited help when irregular water boundaries are involved for two reasons. First, real world water boundaries are of great variability, and only two types of them can be simulated in the laboratory: 1) shallow water with a horizontal or sloped flat bottom and 2) a channel with piercing or submerged sidewalls with particular profiles. Also, in a towing tank, the motions of interacting vessels are typically limited to those parallel to a bank.

Numeric methods might be less accurate, but they have no restrictions on the geometry of water boundaries or the motions of vessels as with experimental methods. This particular advantage makes them the most feasible approach to study the hydrodynamic interaction problem involving irregular water boundaries.

Among all the numerical methods for studying the hydrodynamic interaction problem, RANSE-based real fluid computational methods, for instance, the work of Yang et al [10], and perfect fluid free-surface methods [3] can produce estimates fairly close to experimental results, but neither of them is suitable for online simulations. In contrast, the double-body potential-flow methods are less accurate but fast enough to be run in real time and can still capture the main effect of ship hydrodynamic interaction [11].

An implementation based on the Classic Hess and Smith panel method [12, 13] aiming at real-time simulation was devised by Sutulo and Guedes Soares first for the deep water case [14], and in [9] the code was fused with the manoeuvring simulation program. The interaction code was also validated against available experimental data [15] and compared with field methods [16]. To lift the limitation of a horizontal flat bottom required by the mirror image technique, the panelled moving patch technique was proposed by Zhou et al. [17], which presumes a distribution of a layer of sources both on the wetted surface of each ship and on a part of the seabed. The patches move and turn together with their own associated ships and are dynamically re-meshed during the interaction process. The agreement achieved in the validation of the panelled moving method against the mirror image technique for the horizontal case was very satisfying, but the seabed patches were dynamically discretized by using square-shaped elements of uniform sizes. Obviously, such rigid meshes cannot be successfully used for complex topographies.

Recently an in-house mesh generator has been developed and incorporated with interaction code previously devised to deal ship hydrodynamic interaction problems with arbitrary seabed topographies. In the present paper, the behaviour of the classic panel method with

dynamically generated generic quadrilateral meshes is examined and discussed comparing it with the mirror image technique for a case where both methods are applicable, i.e. in shallow water with the constant depth. Then, two cases involving complex water boundaries are simulated using the panelled moving patch method. Finally, some concluding remarks on the proposed method are drawn.

2. PROBLEM STATEMENT AND THEORETICAL FORMULATION

Consider the global coordinate system $O\xi\eta\zeta$, with the ξ -axis laid on the undisturbed water surface, the ζ -axis directed vertically downwards, and the η axis defined by right-handed convention. The instantaneous advance ξ_{Ci} , transfer η_{Ci} , and the heading angle ψ_i of the i^{th} ship are defined with the help of the body-fixed frame $C_i x_i y_i z_i$ attached to the vessel in question, with its origin located at the mid-ship, the x -axis pointing to the bow, y -axis to the starboard, and the z -axis downwards. A layer of sources is distributed on the wetted surface of each ship and also on a moving patch of a sufficient size placed on the seabed right beneath each ship in question to express the local geometry of the seabed. Under the assumption of sufficiently low Froude number, the mirror-image principle is applied to the undisturbed free surface, then fluid domain is defined by the doubled hull and the panelled moving patch is considered. The total velocity potential Φ takes the form:

$$\Phi = V_{\xi_{cur}} \xi + V_{\eta_{cur}} \eta + \phi, \quad (1)$$

where $V_{\xi_{cur}}$ and $V_{\eta_{cur}}$ are the components of the current velocity in the global axes, and $\phi = \phi(\xi, \eta, \zeta, t)$ is the perturbation potential. Then the induced velocity is:

$$\mathbf{V}_I = \nabla \phi. \quad (2)$$

At any time moment, the perturbation potential should satisfy the Laplace equation

$$\Delta \phi = 0 \quad (3)$$

and on the ship wetted surface and on the moving patch, the following non-penetration boundary condition is applied:

$$\frac{\partial \phi}{\partial n} = \mathbf{V}_r \cdot \mathbf{n}, \quad (4)$$

where \mathbf{n} is the outward unity normal to the local geometry, \mathbf{V}_r is the relative local velocity:

$$\mathbf{V}_r = \mathbf{V} - \mathbf{V}_{cur}, \quad (5)$$

where V is the absolute local velocity on the body surface and on the moving patch.

In the mirror image method, the ships' wetted surfaces constitute the total surface S in the following equations:

$$2\pi\sigma(M) + \int_S \sigma(P) \frac{\partial G(M, P)}{\partial n_M} dS(P) = f(M), \quad (6)$$

where σ is the source density, $M(x, y, z)$ is the field point, $P(x', y', z')$ is the source point belonging to the surface S , and $G(\cdot)$ is the Green function:

$$G(x, y, z, x', y', z') = \sum_{k=0}^n \left(\frac{1}{r_k} + \frac{1}{\bar{r}_k} \right), \quad (7)$$

where $r = \sqrt{(x-x')^2 + (y-y')^2 + (z+kh-z')^2}$, and $\bar{r} = \sqrt{(x-x')^2 + (y-y')^2 + (z+kh+z')^2}$, k is the number of images, and h is the water depth.

The major difference in formulation between the panelled moving patch and the mirror image method is that in the moving patch implementation the total surface S in equation (6) is comprised of both the wetted hull surfaces and the moving patches on the seabed chosen in the vicinity of the ships, and no images are used. Thus the number of images k in equation (7) is zero.

Once the equation (6) is solved, the induced velocity $V_i(M)$ and induced potential $\phi(M)$ at a point M can be obtained by integrating the contribution of each panel:

$$\begin{aligned} V_i(M) &= \int_S \sigma(P) \nabla_M G(M, P) dS(P), \\ \phi(M) &= \int_S \sigma(P) G(M, P) dS(P). \end{aligned} \quad (8)$$

The pressure distribution on the ship hulls can then be calculated using the unsteady Bernoulli equation [18]:

$$p = \rho \left[-\frac{\partial \phi}{\partial t} + \frac{1}{2} (V_r^2 - V_p^2) \right], \quad (9)$$

where

$$V_p = V_i - V_r. \quad (10)$$

The total hydrodynamic inertial force F_{pi} and moment M_{pi} can be calculated by:

$$F_{pi} = -\int_{S_i} p n dS; \quad M_{pi} = -\int_{S_i} p r \times n dS. \quad (11)$$

and their components in the body axes are: the surge force X_p , sway force Y_p , and yaw moment N_p , respectively.

The proper hydrodynamic inertial forces and moments can be expressed as [14]

$$\begin{aligned} X_e &= -\mu_{11}\dot{u} + \mu_{22}vr, \\ Y_e &= -\mu_{22}\dot{v} - \mu_{26}\dot{r} - \mu_{11}ur, \\ N_e &= -\mu_{26}\dot{v} - \mu_{66}\dot{r} + (\mu_{11} - \mu_{22})uv - \mu_{26}ur. \end{aligned} \quad (12)$$

where μ_{ij} are the added mass coefficients. Finally the pure interaction loads are:

$$X_I = X_p - X_e; \quad Y_I = Y_p - Y_e; \quad N_I = N_p - N_e. \quad (13)$$

3. NUMERICAL IMPLEMENTATION AND CONSIDERATIONS

The solution to the equation (6) relies on the discretization of the total surface S into a number of primary elements [12, 13]. For the present problem, the geometric definitions of two surfaces are loaded into the system prior to the simulation of a hydrodynamic interaction process: 1) the wetted surfaces of the interacting ships and 2) the topography of any complex flow boundaries of the restricted waters in which the ship-ship interaction will occur, like canal, banks, or jetties. The former are pre-discretized and will remain the same throughout the entire simulation process, while the latter is loaded unmeshed in the global coordinate system.

When specifying the sizes of the seabed patches associated with the interacting vessels, a trade-off must be made between the accuracy of the numerical results and the computation speed. With the same panel density, a larger size of the patch may result in better accuracy but will significantly increase the computation speed. On the other hand, the patch must be sufficiently large so as to obtain acceptable accuracy. It had been established in the earlier study [17] that the patch with area approximately equal to $17A_w$ is sufficient and patches of this size are also used in this study.

To determine whether the two seabed patches are intersecting when the two interacting ships come close to one another, a standard point-in-polygon algorithm is used and run for each vertex of either patches. However, if the maximum value of any coordinate of any patch is less than the minimum value of the corresponding coordinate.

In case of an interaction occurring near a shoreline, when not the entire patch is in the water, the part outside water is trimmed to the fluid boundary with a polygon-clipping procedure based on the Sutherland-Hodgman algorithm [19].

In the actual interacting process between two manoeuvring vessels moving on arbitrary courses, the resultant unified patches may form a polygon containing very short sides with lengths much smaller than the desired panel size. This situation should be avoided because it challenges both the mesh smoothing procedure and the Gauss-Seidel iteration

invoked afterwards to solve the set of equations for the source densities. For instance, the patch union under the two interacting ships shown in Figure 1 contains a very short side $\overline{N_3N_4}$, which will cause elements unbalanced in size in the local region and result in panels of poor quality (very small of interior angles, large size ratios, etc.) hard to be optimized if the meshing is carried out unconditionally. Besides the latent possibility of producing panels of inferior quality, an extra short side will certainly lead to panels with sizes much smaller than average panel size that can also stall the iterative process.

A possible remedy for the short side $\overline{N_3N_4}$ in Figure 1 is to use a surrogate side $\overline{N_3'N_4'}$ for a new local meshing boundary. Remedying short sides may introduce some undesired numerical noise in the solution, but removes hassles to the solver.

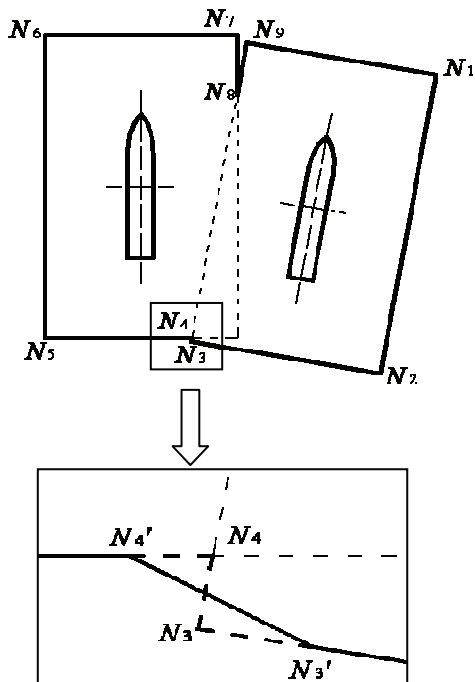


Figure 1. Remedy of extra short sides contained in the patch union of two interacting ships

In order to simulate online, a second trade-off is to be made on the panel density. For a patch of a given size, a higher grid refinement will help produce more accurate results but also increase the computation time which is approximately proportional to n^2 with the Gauss–Seidel iteration method.

In this work, the panel sizes of the seabed patches are comparable to those used on the ship hulls, namely, an average diagonal of 8 meters (about $\frac{1}{4}$ of the beam of the ship). Higher refinement in the central regions of the patches may increase the accuracy of the results [20] at least when the patches are only discretized into rectangular elements, but that must

be done either by subdividing mesh regions or through meshing with constraints [21] which will incur more difficulty in meshing the patches and this must be preceded by the validation of the method with generic quadrilateral meshes.

Once the seabed patch union and the panel size are determined, an in-house mesh generator based on the paving algorithm [22] is invoked to discretize it into quadrilateral elements. The so-called paving algorithm is an advancing front meshing method which starts meshing from the nodes predefined on the geometry boundaries (Note that in this context a boundary, unlike its definition in describing a fluid domain where it refers to a surface that encloses a volume in space, is a circuit of line segments by which a non-closed surface is bounded). New elements are created according to the boundary nodal configurations and properly placed from the boundary toward the interior. The paving boundary or the advancing front is being updated as new elements are inserted. The paving boundaries are advanced alternatively if there is more than one boundary. When intersections of the paving boundaries (including self-intersections) are detected, an intersection handling module is invoked to connect the fronts and, depending on the situation, to merge two paving boundaries or split one boundary into two or more. This process continues until all the paving boundaries are closed. Figure 2 shows an example of meshing a rectangle plate with a hole in it, where the arrows show the directions in which the elements are installed along the exterior and interior geometry boundaries respectively.

In all simulations presented below, the required panel refinement was obtained online with the help of the algorithm described above. The obtained grids were further improved with a hybrid smoothing algorithm combining the Lagrange smoothing [22] and the angle-based technique [23] to bring the interior angles of each panel to the interval from 30 to 150 degrees.

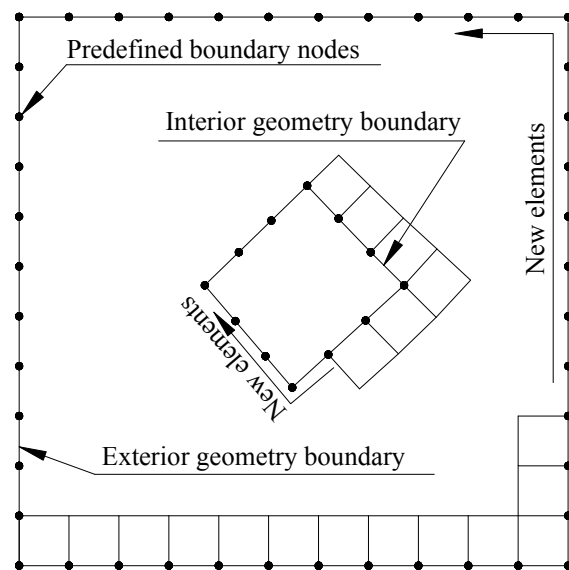


Figure 2. The mechanism of the paving algorithm

4. VALIDATION FOR CONSTANT DEPTH

In fact, a reasonable agreement between the moving patch method and the mirror image method has already been demonstrated for the unbounded case with all rectangular patches [17], while in the present article, this is performed for dynamically generated grids.

A purely kinematic (i.e. without any dynamic feedback) simulation of an overtaking manoeuvre on parallel courses was carried out for two ships in shallow water with a constant depth of 14 meters. The two ships have an identical ship form with dimensions $L \times B \times T$ of $189.6\text{m} \times 31.6\text{m} \times 10.3\text{m}$. Ship 1, referred to as the overtaking ship hereafter, is moving at 3m/s at the port side of Ship 2 being overtaken with a constant lateral distance of 36 meters between the centreplanes.

The results, together with the deep-water data given for comparison, are presented in Figures 3 through 8 as functions of the instantaneous non-dimensional longitudinal shift

$$\xi' = \frac{\xi_1 - \xi_2}{L_1 + L_2}, \quad (14)$$

where ξ_1 and ξ_2 are the advances of overtaking and overtaken ships respectively and the hydrodynamic interaction forces are also presented in the non-dimensional form:

$$\begin{aligned} F_i' &= \frac{2F_i}{\rho L_i T_i (V_1^2 - V_1 V_2 + V_2^2)}, \\ M_i' &= \frac{2M_i}{\rho L^2 T_i (V_1^2 - V_1 V_2 + V_2^2)} \end{aligned}, \quad (15)$$

where V_i is the velocity of the i^{th} ship. A somewhat complicated reference velocity

$$V_{ref} = \sqrt{V_1^2 - V_1 V_2 + V_2^2} \quad (16)$$

is chosen in such a way that it reduces to intuitively consistent with most typical specific cases: i.e. when $V_1 = V_2$, $V_1 = 0$, or $V_2 = 0$

Some ‘noise’ is present on almost all the time histories in the case of the panelled moving patch method, especially for the overtaking ship that has a higher velocity. The explanation for this phenomenon is that the induced velocity or the pressure, evaluated at the control point (centroid) of the panel is taken as the value for any point elsewhere on the panel; such a uniform representation of quantities creates an error with the actual distributions in a pattern specific to the geometric characteristics of the panel for a given flow state, and this error pattern remains the same or similar at the next time instant if the

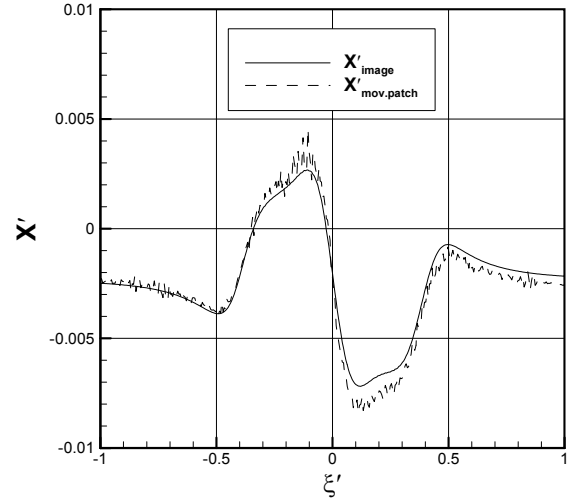


Figure 3. Surge force acting on the ship overtaking another in shallow water

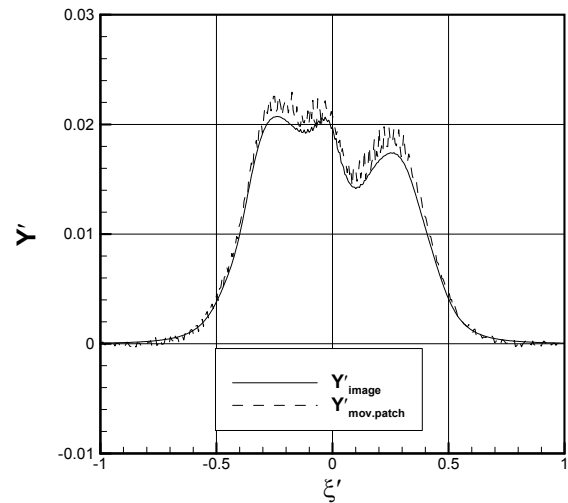


Figure 4. Sway force acting on the ship overtaking another in shallow water

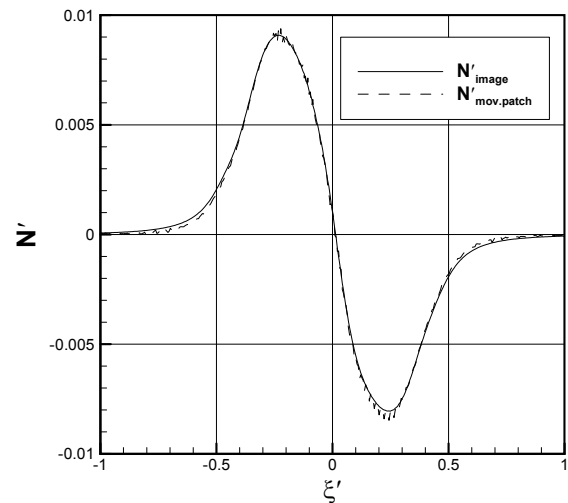


Figure 5. Yaw moment acting on the ship overtaking another in shallow water

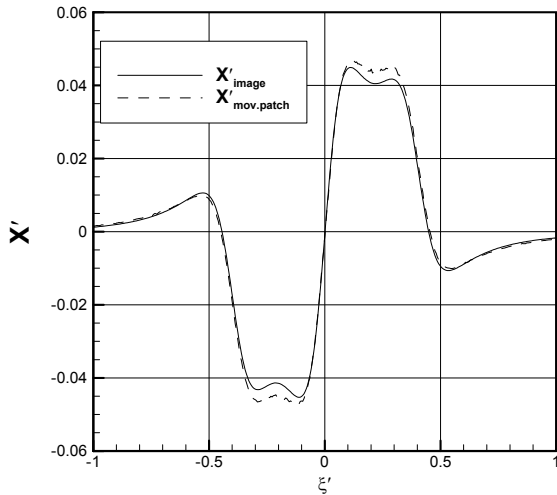


Figure 6. Surge force acting on the ship overtaken by another in shallow water

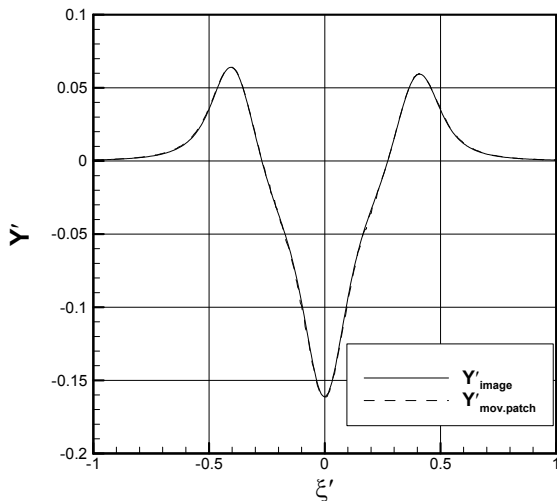


Figure 7. Sway force acting on the ship overtaken by another in shallow water

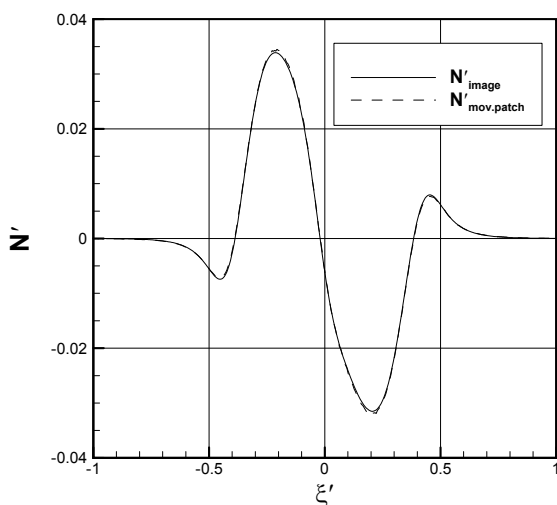


Figure 8. Yaw moment acting on the ship overtaken by another in shallow water

geometric characteristics do not change and provided the change of flow properties between the two instants is relatively small. This is why the mirror image technique which is also implemented with the same panel method, (although on the hulls only), does not present obvious noise in its numerical results but the panelled moving patch method does because the seabed meshes at two consecutive time instants lack similarity of geometric characteristics. Fortunately, the numerical noise did not swallow the actual solution and forces, in general, are still correctly presented by the method.

5. HYDRODYNAMIC INTERACTION BETWEEN SHIPS MOVING IN CONFINED WATERS WITH COMPLEX BOUNDARIES

As was already commented, the moving patch method can be applied for arbitrary bathymetry, two cases involving arbitrary seabed topography are studied: 1) ship encountering inside a canal which is a typical ship-ship interaction scenario inside canals and 2) ship overtaking over a dredge channel which is often seen around harbours and ports.

5.1 SHIP ENCOUNTER INSIDE A CANAL

The same as in the simulation in the validation, the two ships have the same form previously described. Both ships have the same constant lateral distance from their own centreplanes to the central line of the channel which is 18 meters, and they both are moving in parallel courses at a speed of 2m/s but in opposite directions. The canal has a water depth of 14 meters a width of 80 meters at its bottom and 90 meters at the top of the sloped banks, see Figure 9. As the ships are identical, the time histories are only presented for Ship 1 in Figures 10 through 12 where are also presented for comparison the time histories for the same overtaking simulation but in unbounded shallow water of 14 meters of constant depth.

The sway force time history curve starts at a value significantly different from zero, as seen in Figure 11.

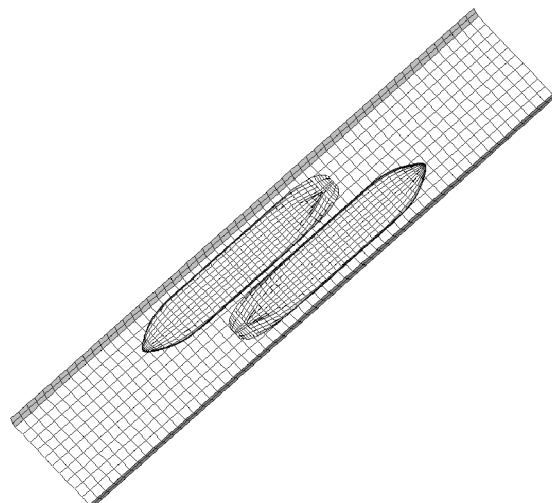


Figure 9. Ship encounter in a canal

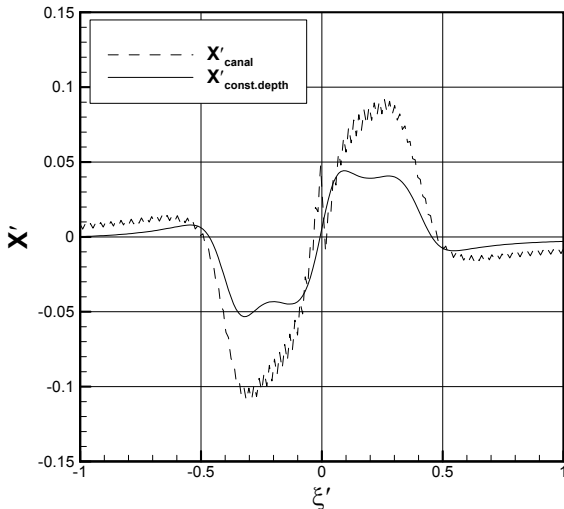


Figure 10. Surge force acting on the ship in the event of an encounter in a canal

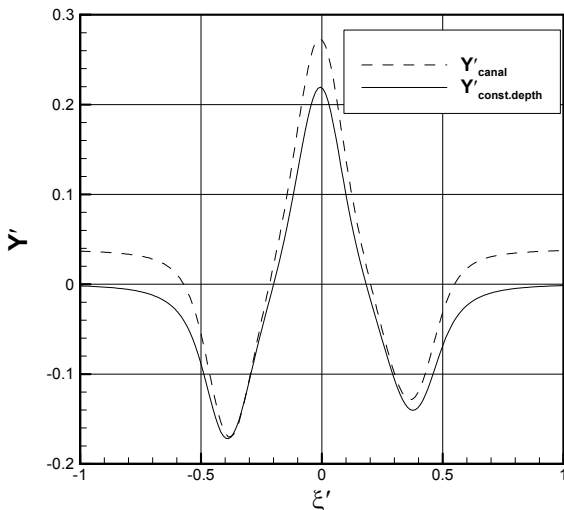


Figure 11. Sway force acting on the ship in the event of an encounter in a canal

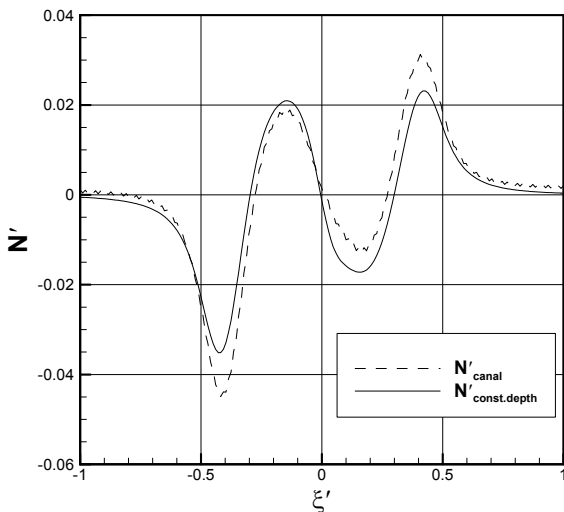


Figure 12. Yaw moment acting on the ship in the event of an encounter in a canal

This happens due to the bank effect, and this part of the sway force will accompany any off-centred motions. However, a similar effect practically is not shown for the surge force and the yaw moment as the difference in shape form between the fore body and the aft body is very small and consequently the yaw moments generated by the two semi-bodies approximately cancel each other.

Except for the surge force which is usually of smaller magnitude and more difficult to estimate numerically, both the sway force and the yaw moment have rather smooth time history curves, that is because the only change in geometric characteristics of the patch union was the total length and for which the mesh generator produced all square-shaped elements that always shared geometric similarities. As a result, the numerical noise discussed before was insignificant in this case.

5.2 SHIP OVERTAKING OVER A DREDGED CHANNEL

In this simulation, the dredged channel is 80 meters wide at its bottom and 90 meters wide at the surrounding seabed level. The water depth is 18 meters inside the channel and 13 meters outside it. Smaller panels are used on the sloped channel walls in order to create at least two rows of elements as it is difficult for the mesh smoother to refine a grid containing only a single row of elements. See Figure 13. The ship on the left hand side is moving at 3m/s overtaking the other ship moving at 1 m/s. The ships are moving on parallel courses and intersect the channel's axis at 45 degrees. The constant lateral distance between the two ships' centreplanes is 36 meters.

The time histories are plotted in Figures 14 through 16 and in Figures 17 through 19 for the overtaking and the overtaken ships respectively. The overtaking ship has responses for both the surge and sway forces very different from those in constant depth, while no significant difference is exhibited for the yaw moment. For the overtaken ship, the obtained curves are in general smoother than those of the overtaken ship because of the lower speed. Another interesting observation for the overtaken ship is that the peak values of all the forces components are smaller in the dredged channel case than in the constant water depth case.

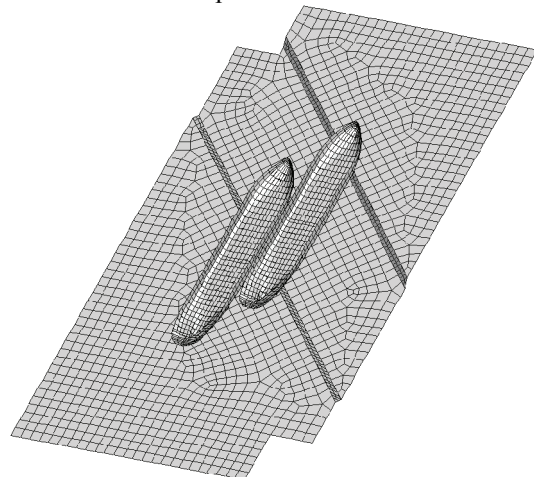


Figure 13. Ship overtaking over a dredged channel

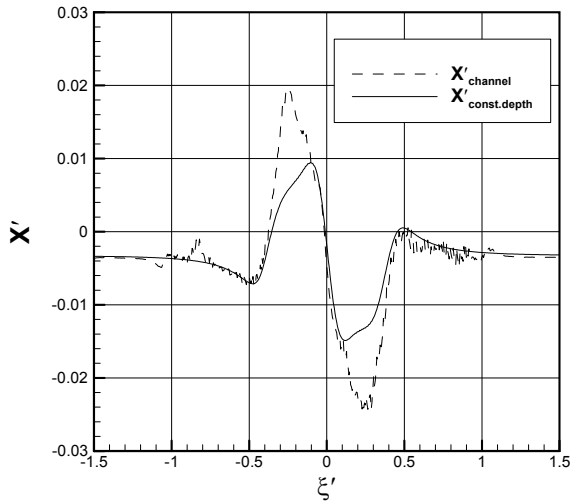


Figure 14. Surge force acting on the ship overtaking another ship over a dredged channel

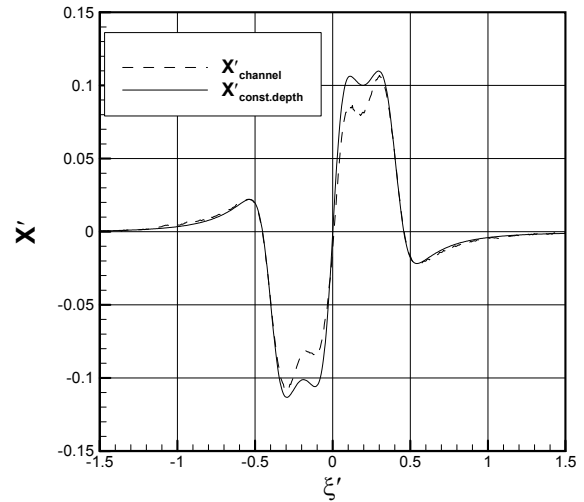


Figure 17. Surge force acting on the ship being overtaken by another ship over a dredged channel

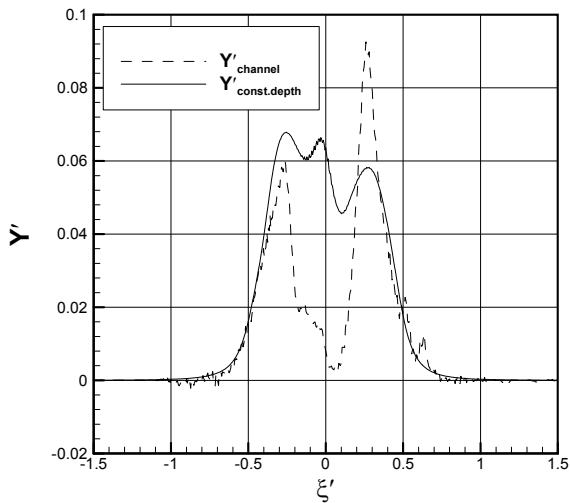


Figure 15. Sway force acting on the ship overtaking another ship over a dredged channel

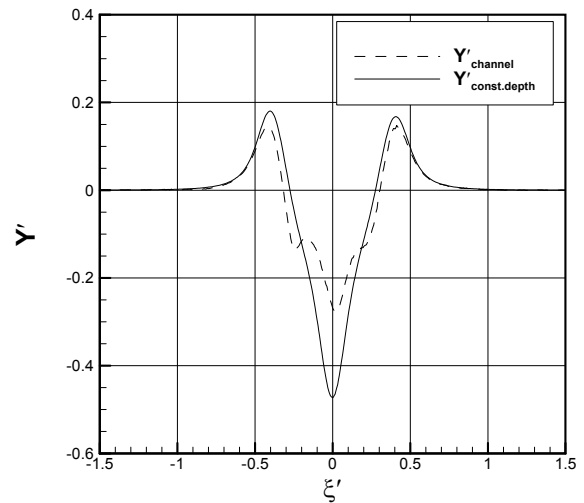


Figure 18. Sway force acting on the ship being overtaken by another ship over a dredged channel

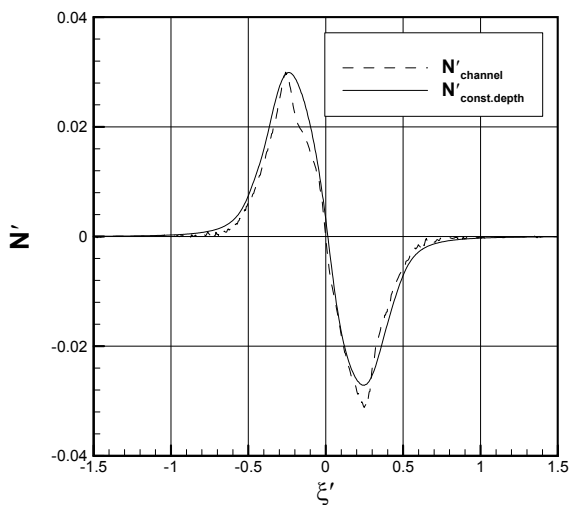


Figure 16. Yaw moment acting on the ship overtaking another ship over a dredged channel

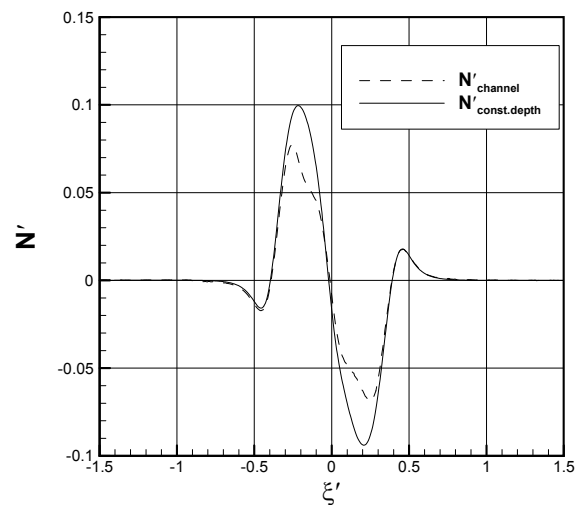


Figure 19. Yaw moment acting on the ship being overtaken by another ship over a dredged channel

6. CONCLUSIONS

A complete solution to the real time estimation of hydrodynamic interaction between manoeuvring ships in restricted waters with complex boundaries is presented, in which the complex seabed topography is dealt with the proposed moving patch method. Numerical behaviour of the method has been investigated for the case of generic quadrilateral meshes dynamically generated with the integrated meshing algorithm.

Validation against the mirror image technique has shown that the method can produce results with satisfactory accuracy and is now suitable for practical simulations of hydrodynamic interaction loads on manoeuvring ships in restricted waters with complex boundaries. The motions of the interacting ships are no longer limited to be parallel.

Although the numerical noise is in general small and most interaction forces can be correctly estimated with the method, but it may appear in various real-world ship-ship interaction scenarios in confined waters simply because the meshes generated at two consecutive time instants lack geometric similarities. A better formulation is to be made in order to remove or reduce the numerical errors.

7. ACKNOWLEDGEMENTS

This work was performed within the project “Energy Efficient Safe Ship Operation (SHOPERA)” funded by the European commission under contract No.605221. The first author was supported by Portuguese Foundation for Science and Technology (Fundação para a Ciência e Tecnologia) under contract no. SFRH/BD 75354/2010.

8. REFERENCES

1. LAFORCE E., CLAEYSSENS P., VANTORRE M. Influence of the Ship's Length on the Maneuverability in a Canal. *Proceedings of the 11th International Harbour Congress, Antwerpen, Belgium*, pp 523–534. (1996)
2. KYULEVCHELIEV S., GEORGIEV S., IVANOV I. Hydrodynamic Interaction between Moving and Stationary Ship in a Shallow Canal. *Third international conference on port development and coastal environment PDCE, Varna, Bulgaria*. (2003)
3. SÖDING H., CONRAD F. Analysis of Overtaking Manoeuvres in a Narrow Waterway. *Ship Technology Research, Vol. 52*, pp 189–193. (2005)
4. GRONARZ A. Ship-Ship Interaction: Overtaking and Encountering of Inland Vessels on Shallow Water. *Proceedings International Conference on Marine Simulation and Ship Manoeuvrability (MARSIM'06), 25–30 June 2006, Terschelling, The Netherlands*, pp M-1-1–M-1-5. (2006)
5. VANTORRE M., DELEFORTRIE G., ELOOT K., LAFORCE E. Experimental Investigation of Ship-Bank Interaction Forces. *Proceedings International Conference on Marine Simulation and Ship Maneuverability (MARSIM'03), 25–28 August 2003, Kanazawa, Japan, Vol. 3*, pp RC-31-1–RC-31-9. (2003)
6. VANTORRE M., VERZHBITSKAYA E., LAFORCE E. Model Test Based Formulations of Ship-Ship Interaction Forces. *Ship Technology Research. Schiffstechnik, Vol. 49*, pp 124-141. (2002)
7. VARYANI K. S., VANTORRE., M. Development of New Generic Equation for Interaction Effects on A Moored Container Ship Due to Passing Bulk Carrier. *International Journal of Maritime Engineering, Vol. 147, Part A2, June, 2005 11*. (2005)
8. FALTER J. Validation of a Potential Flow Code for Computation of Ship-Ship Interaction Forces with Captive Model Test Results. *Master Thesis in Naval Architecture and Marine Engineer. IST, Lisbon University*. (2010)
9. SUTULO S., GUEDES SOARES C. Simulation of Close-Proximity Maneuvers Using an Online 3D Potential Flow Method. *Proceedings of International Conference on Marine Simulation and Ship Manoeuvrability (MARSIM'09), Panama City, Panama, 17-20 August*, pp M-9-1–M-9-10. (2009)
10. YANG H., WU B.S., MIAO Q.M., XIANG X., BERG T.E., KUANG X.F. Study on the Effects of Unsteady Ship to Ship Interaction by CFD method. *Proceedings of the 2nd International Conference on Ship Manoeuvring in Shallow and Confined Water: Ship to Ship Interaction*. May 18–20, Trondheim, Norway, pp. 393–398. (2011)
11. TUCK E. O., NEWMAN J. N. Hydrodynamic Interactions between Ships. *Proceedings of the 10th Symposium on Naval Hydrodynamics, Cambridge, Mass., USA*, pp 35–69. (1974)
12. HESS J.L., SMITH A.M.O. Calculation of Nonlifting Potential Flow about Arbitrary Three-Dimensional Bodies. *Journal of Ship Research*. 8, pp 22–44. (1964)
13. HESS J.L., SMITH A.M.O. Calculation of Potential Flow about Arbitrary Bodies. *Progress in Aeronautical Sciences, 8*, pp 1–137. (1967)
14. SUTULO S., GUEDES SOARES C. Simulation of the Hydrodynamic Interaction Forces in Close-Proximity Manoeuvring. *Proceedings of the 27th Annual International Conference on Offshore Mechanics and Arctic Engineering, Estoril, Portugal, 15–19 June, Paper OMAE2008-57938*. (2008)
15. SUTULO S., GUEDES SOARES C., OTZEN J.F., Validation of Potential-Flow Estimation of Interaction Forces Acting upon Ship Hulls in

- Side-to-Side Motion. *Journal of Ship Research*, Vol.56, Issue 3, pp. 129–145. (2012)
16. FONFACH J.M.A., SUTULO S., GUEDES SOARES C. Numerical Study of Ship-to-Ship Interaction Forces on the Basis of Various Flow Models. *Proceedings of the 2nd International Conference on Ship Manoeuvring in Shallow and Confined Water: Ship to Ship Interaction*. May 18-20, Trondheim, Norway. pp. 137–146. (2011)
 17. ZHOU X-Q., SUTULO S., GUEDES SOARES C. Computation of Ship-to-Ship Interaction Forces by a 3D Potential Flow Panel Method in Finite Water Depth. *Journal of Offshore Mechanics and Arctic Engineering*. Vol. 136. pp 041301-1 – 041301-8, (2014).
 18. LAMB H. *Hydrodynamics*, Dover Pub, New York. (1968)
 19. SUTHERLAND I. E., HODGMAN G. W. Reentrant Polygon Clipping. *Communications of the Association for Computing Machinery*, 17(1) January, pp 32–42. (1974)
 20. ZHOU X-Q., SUTULO S., GUEDES SOARES C. Computation of Ship Hydrodynamic Interaction Forces in Restricted Waters Using Potential Theory. *Journal of Marine Science and Application*, vol. 11, pp 265–275. (2012)
 21. PARK C., NOH J-S, JANG I., KANG J.M. A New Automated Scheme of Quadrilateral Mesh Generation for Randomly Distributed Line Constraints. *Computer-Aided Design* 39, pp 258–267. (2007)
 22. BLACKER T.D., STEPHENSON M.B. Paving: A New Approach to Automated Quadrilateral Mesh Generation. *International Journal for Numerical Methods in Engineering*., vol. 32, pp 811–847. (1991)
 23. ZHOU T., SHIMADA K. An Angle-Based Approach to Two-Dimensional Mesh Smoothing. *Proceedings of the 9th International Meshing Roundtable*. pp 1–12. (2000)